Characterization of potential biophysical regulators for clustering of the multifunctional lipid PI(4,5)P_2

Raquel Alexandra Bispo Guerreiro

Thesis to obtain the Master of Science Degree in
Biotechnology

Supervisor: Dr. Fábio Monteiro Fernandes; Co-Supervisor: Dr.Sandra Cristina Nunes Trigo Fernandes Pinto

ABSTRACT

PI(4,5)P_2 is an important phospholipid found in the inner leaflet of the plasma membrane of eukaryotes. PI(4,5)P_2 has a high affinity for Ca^{2+} and in its presence forms clusters on lipid membranes. Very recently, studies have revealed the role of PI(4,5)P_2 in yeast response to osmotic shock. These results revealed a previously unidentified function of PI(4,5)P_2 as a plasma membrane tension sensor. The behaviour of PI(4,5)P_2 in this mechanism is highly unexpected for monomeric PI(4,5)P_2 and could be associated with the aggregated pool of PI(4,5)P_2 in the plasma membrane. Saturated PI(4,5)P_2 was also recently shown to generate gel phase domains in the presence of calcium, even at very low levels. While conventional gel domains are disrupted by cholesterol, the role of this sterol in the formation of PI(4,5)P_2-based gel domains was unknown. Using a combination of fluorescence spectroscopy and microscopy, we demonstrate that membrane tension had no impact on PI(4,5)P_2 clustering, while cholesterol was inefficient in disrupting the gel phase formation by saturated PI(4,5)P_2. Additionally, PI(4,5)P_2 clustering was also shown to be unresponsive to temperature in the range of 20-70°C. These results suggest that PI(4,5)P_2 clustering is not prone to regulation.

Keywords: PI(4,5)P_2**;** Calcium; Membrane tension; Cholesterol

1. Introduction

PI(4,5)P_2 is the most abundant phosphoinositide in mammalian cells and is found primarily in the inner leaflet of the plasma membrane[1]. PI(4,5)P_2 can interact, recruit and/or regulate a variety of signalling proteins. It plays a central role in several processes, including cell adhesion and motility[2] vesicle endocytosis and exocytosis and ion channel transport[3].

PI(4,5)P_2 are able to establish strong electrostatic interactions between their negatively charged headgroup and positively charged proteins or divalent cations. In the cellular PI(4,5)P_2 context, calcium (Ca^{2+}) and magnesium (Mg^{2+}) stand out as relevant binding partners[1]. Both divalent cations have been shown to bind strongly to PI(4,5)P_2 and influence its lateral organization[1].

The addition of Ca^{2+} was shown to induce PI(4,5)P_2 clustering within physiological levels in liposomes[4].

Furthermore, in membranes containing cholesterol, Ca^{2+} seems to favour partition of PI(4,5)P_2 molecules to raft-like domains, where clustering seems to be more efficient. Ca^{2+} may even potentiate protein anchoring in cholesterol-enriched domains, by increasing PI(4,5)P_2 density in these microdomains[5].

Plasma membrane tension is used to control multiple cellular events. The sensors of PM tension were until recently generally thought to be transmembrane proteins or peripheral membrane proteins, including stretch-activated ion channels, curvature-sensing proteins or membrane interacting proteins[6]. Membrane–cytoskeleton and osmotic pressure can also contribute to PM tension[6]. The target of rapamycin complex 2 (TORC2) plays a vital role in maintaining the homeostasis of the PM tension[7].TORC2 is recruited to the PM through binding to PI(4,5)P_2[7]. Recent studies have shown that a decrease in the membrane tension triggers PI(4,5)P_2 phase separation into membrane invaginations and leads to co-clustering of TORC2 with PI(4,5)P_2 within these areas, with concomitant inactivation of TORC2[7]**.** Strikingly, the results regarding the relationship between PI(4,5)P_2 distribution and membrane tension presented the interesting possibility that PI(4,5)P_2 is the primary molecular sensor of decreased PM tension, with further activation/deactivation of PM membrane tension sensors acting just as responses to this initial and possibly spontaneous event [7].

$PI(4,5)P_2$ is an important regulator of lipid metabolism in response to thermal stress. Thus, a drop in temperature reduces $PI(4,5)P_2$ levels and so the activity of some essential signalling effector in response to cold[8]. The dramatic increase in surface area with temperature was hypothesized to be associated with a disruption of the hydrogen boding network as temperature increases. In this case, the structure of $PI(4,5)P_2$ clusters is expected to show considerable differences at different temperatures.

$PI(4,5)P_2$, was show to favourably partition into the liquid disordered phase (cholesterol depleted) of the lipid bilayer due to its large negatively charged headgroup and highly unsaturated acyl chain[1]. Surprisingly, this preference was largely disrupted in the presence of divalent cations, which at very high concentrations even induced a shift in partition to a moderate preference for liquid-ordered phase[5].

Saturated $PI(4,5)P_2$ were recently show to cluster into gel phase domains, even when present at very low concentrations in the membrane (~1%)[9]. The high cholesterol concentration at the plasma membrane of animal cells shifts the threshold for gel phase formation to a concentration of gel triggering lipids that is considerably above their natural abundance. This effect is of critical importance for cell viability. However, in the case of saturated $PI(4,5)P_2$, gel phase formation is mostly triggered by segregation of the lipids due to headgroup interactions, and not due to acyl-chain packing preferences as seen for other lipid classes .In this way, it is not clear if cholesterol could prevent the formation of such phases. If not, the prevalence of the polyunsaturated canonical $PI(4,5)P_2$ specie, which evolution favoured, could have risen as a mechanism to prevent the formation of solid $PI(4,5)P_2$ domains. Recently, the polyunsaturated canonical $PI(4,5)P_2$ specie inhibited was also shown to inhibit the formation of gel phase by the saturated $PI(4,5)P_2$, supporting this hypothesis[9].

2. Materials and Methods

2.1 Materials

1-Palmitoyl-2-oleoyl-*sn*-glicero-3-phosphocholine (POPC), 1,2-dioleoyl-*sn*-glycero-3-phospho-(1'-myo-inositol-4',5'-bisphosphate) (di18:1PI(4,5)P2), 1-stearoyl-2-arachidonoyl-*sn*-glycero-3-phospho-(1'-myo-inositol-4',5'-bisphosphate)(18:020:4$PI(4,5)P_2$), 1-oleoyl-2-{6-[4 (dipyrromethene borondifluoride) butanoyl]amino}hexanoyl-*sn*-glycero-3-phosphoinositol-4,5-bisphosphate (TopFluor $PI(4,5)P_2$), and 1,2-dioleoyl-*sn*-glycero-3-phosphoethanolamine-N-(cap biotinyl) (DOPE-Cap-biotin. All lipids were purchased from Avanti Polar Lipids (Alabaster, AL, USA). 1,2-Dipalmitoyl-sn-glycero-3-phospho-(1'-myo-inositol-4',5'-bisphosphate) (di16:0 $PI(4,5)P_2$) was from Echelon Biosciences (Salt Lake City, UT, USA). Lipid stock solutions were prepared in chloroform, except for the phosphoinositides, which were prepared in chloroform: methanol (MeOH) 2:1(v/v). Both solvents were obtained from Merck (Darmstadt, Germany) and were of spectroscopic grade. Ethanol (EtOH), NaCl, Sucrose, EDTA, glucose and $CaCl_2$ were from Sigma-Aldrich (St. Louis, MO, USA). Trans-parinaric acid, DOPE-Rhodamine and Fluo-5N were from Molecular Probes, Invitrogen (Eugene, OR, USA). Avidin egg white and cholesterol (chol) were from Sigma Chemical Co. (St. Louis, MO). All organic solvents were UVASOL grade from Merck Millipore (Darmstadt, Germany).

2.2 Lipossome preparation

Large unilamellar vesicles (LUVs) were prepared by extrusion of multilamellar vesicles. The lipid mixtures were prepared from phospholipid stock solutions. The solvent was slowly vaporized under a nitrogen flux and the resulting lipid film was left in vacuum for 3 hours to ensure the complete removal of the organic solvent. Afterwards, the lipid was re-suspended in a solution of sucrose. Freeze-thaw cycles were performed, using liquid nitrogen and a water bath typically set to 60 ºC. LUVs were finally obtained by extrusion of the solutions at room temperature with an Avanti Mini-Extruder (Alabaster, AL) using 100 nm pore size polycarbonate membranes.

GUVs were obtained by gel-assisted formation and by electroformation in Pt wires, both based on previously described methods[10,11].

In the case of gel-assisted vesicle formation, the lipid mixtures were prepared, from stock solutions, in chloroform to a final concentration of 1.5 mM. These were composed of 95% POPC and 5% PI(4,5)P2.

The solvent was evaporated for 15 minutes under vacuum. After evaporation of the solvent, the appropriate solution with 200 mM sucrose was added, allowing for GUV formation for 60 minutes at room temperature. After the formation, GUVs were transferred to a µ-slide chamber with the appropriate coating.

For the electroformation, lipid solutions were prepared in chloroform (from lipid stock solutions) in a probe/lipid ratio of 1/500 (mol:mol) for Rho-DOPE, and 1/200 for TF-PI(4,5)P_2. After removal of the solvent, electroformation was performed in 1mL of a 200mM sucrose solution. After formation, GUVs were transferred to a µ-Slide from Ibidi (Munich, Germany) coated with avidin, and a 200 mM glucose solution was also added.

2.3 UV visible spectroscopy

UV-visible absorption measurements were performed using a JASCO V-660 UV-VIS spectrophotometer (JASCO, Tokyo, Japan), at room temperature, using a bandwidth and sampling interval of 1 nm. For the spectrophotometric quantification, quartz cuvettes (Hellma Analytics) with a path length of 1 or 0.5 cm were used.

2.4 Steady-state fluorescence anisotropy

Fluorescence measurements were carried out in a JASCO FP-8500 spectrofluorometer (JASCO, Tokyo, Japan) equipped with a peltier temperature controller and Polarizers. Both fluorescence intensity and fluorescence anisotropy measurements were carried out in quartz cuvettes (Hellma Analytics) having a path length of 0.5 cm. Fluorescence intensity values of TF-PI(4,5)P_2 were recovered from the integration of fluorescence emission spectra obtained with an excitation of 460 nm. Fluorescence anisotropy values were obtained using 460 and 510 nm for excitation and emission wavelengths, respectively. Steady-state fluorescence anisotropy, ⟨r⟩ is defined as:

$$< r >= \frac{I_{VV} - GI_{VH}}{I_{VV} + 2GI_{VH}} \ (1) \ G = \frac{I_{HV}}{I_{HH}} \ (2)$$

Where I_{VV} and I_{VH} are the steady-state vertical and horizontal components of fluorescence emission, respectively, with vertically polarized excitation. The components with horizontally polarized excitation, IHV and IHH, are used to calculate the factor G, present on equation (2):

The *G* factor is the ratio of the system's different sensitivities for vertically and horizontally polarized light and is used to correct fluorescence anisotropy measurements.

2.5 Confocal fluorescence microscopy

Confocal laser scanning fluorescence microscopy measurements were performed on a Leica TCS SP5 (Leica Microsystems CMS GmbH, Manheim, Germany) inverted confocal microscope (DMI600). A 63x apochromatic water immersion objective with a NA 1.2 (Zeiss, Jena Germany) was used for all measurements, and an Argon laser was used for excitation. All analysis of confocal imaging data was carried out using ImageJ.

2.6 Fluorescence lifetime imaging microscopy (FLIM)

Fluorescence lifetime imaging microscopy (FLIM) measurements were performed through time correlated single photon counting (TCSPC) using the same setup of confocal microscopy, coupled to a multiphoton Titanium: Sapphire laser (Spectra- Physics Mai Tai BB, Darmstadt, Germany, 710–990 nm, 100 femtosecond pulses, 80 MHz) as an excitation source. A photomultiplier tube was coupled to the X-port of the microscope and the emitted photons were processed by an SPC board that addresses simultaneously the (x, y) location of the collected photons (Becker and Hickl, GmbH, PMC-100-4 SPC-830). The laser power was adjusted to give an average photon counting rate higher than 5 x 10^4 photons per second and images were acquired for 60 seconds to achieve reasonable photon statistics.

The excitation wavelength was set to 800 nm and emission light was selected using a dichroic beam splitter with an excitation SP700 short-pass filter and an emission 647/75 bandpass filter inserted in front of the photomultiplier for Flipper-TR, and for TF-PI(4,5)P_2 was used dichroic beam splitter with an excitation SP700 short-pass. Images were acquired using a Becker and Hickl SPC 830 module. Fluorescence lifetimes were obtained by analysing the fluorescence decays through a least square iterative re-convolution of decay functions with the instrument response function

(IRF) using the software SPC Image (Becker and Hickl, Berlin, Germany).

2.7 Time-resolved fluorescence spectroscopy

Fluorescence decay measurements were carried out using the time-correlated single-photon timing (TCSPT) technique, as described elsewhere [12]. The emission wavelength was selected by a Jobin Yvon HR320 monochromator (Horiba Jobin Yvon, Kyoto, Japan). 0.5 × 0.5 cm^2 quartz cuvettes from Hellma were used. Blank decays were acquired, and photon counts were negligible. The fluorescence intensity decays were described by a sum of exponentials:

$$i(t) = \sum_i \alpha_i \exp\left(-\frac{t}{\tau_i}\right) (3) \quad \bar{\tau} = \sum_i \alpha_i \tau_i \ (4)$$

where α_i is the normalized amplitude and τ_i is the i^{th} lifetime component. The amplitude-weighted average lifetime is defined as:

Data analysis was performed with the TRFA software (Scientific Software Technologies Center, Minsk, Belarus), based on Levenberg–Marquardt nonlinear least-squares fitting. The goodness of the fit was judged from the experimental χ^2 weighted residuals and autocorrelation plot. In every analysis, χ^2 was below 1.3 and both the residuals and the autocorrelation were randomly distributed around zero.

3. Results

3.1. Electrophoretic Light Scattering

In order to confirm interaction of calcium with $PI(4,5)P_2$ within liposomes, the surface charge of liposomes containing $PI(4,5)P_2$ was evaluated in the presence of different calcium concentrations using electrophoretic light scattering measurements. We prepared LUVs containing 5% $PI(4,5)P_2$ and 95% of POPC in 10, 50 and 100 μM Ca^{2+} buffer, and also in the absence of calcium (5 mM EDTA).

The values of zeta potential recovered for liposomes containing $PI(4,5)P_2$ were less negative than expected, considering the concentration (5%) of the highly anionic lipid. Still, it is possible to notice that liposomes with $PI(4,5)P_2$ at a temperature of 25ºC (Figure 1) have considerably more negative charge when compared to the zwitterionic POPC at the same temperature. In addition, we see that this difference decreases with increasing calcium concentration, due to association of Ca^{2+} with the membrane and $PI(4,5)P_2$ charge neutralization.

These results clearly demonstrate calcium association to the lipid membrane containing $PI(4,5)P_2$. At this lipid concentration, 100 μM of $CaCl_2$ is nearly sufficient for complete surface charge neutralization, suggesting that $PI(4,5)P_2$ are almost saturated with Ca^{2+} ions.

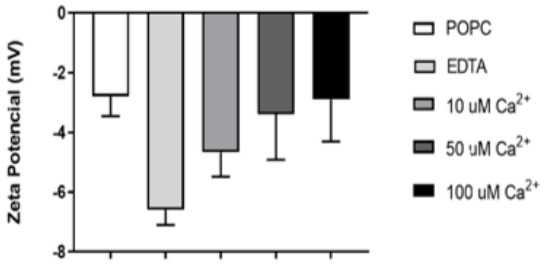

Figure 1 Zetapotencial at 25ºC. The results represent the mean of 3 measurements (N=6), 100 runs each with a equilibration time of 30 seconds in the presence of different calcium concentrations.

3.2. Impact of temperature on calcium-dependent $PI(4,5)P_2$ clustering

Temperature is a strong modulator of lipid membrane structure and dynamics. In the case of calcium-induced $PI(4,5)P_2$ clustering, the importance of temperature for the formation of such structures is still unclear. In order to clarify this issue, fluorescence spectroscopy measurements were carried out with the fluorescent analogue TF-$PI(4,5)P_2$.TF-$PI(4,5)P_2$ was previously shown to incorporate within Ca^{2+}-induced clusters of $PI(4,5)P_2$[4,5] , and clustering of $PI(4,5)P_2$ can be detected by either fluorescence self-quenching or homo-FRET between fluorescent analogues of $PI(4,5)P_2$ (TF-$PI(4,5)P_2$)[4,5].

In order to test the effect of temperature on calcium-induced $PI(4,5)P_2$ clustering we prepared LUVs containing a mixture of POPC:$PI(4,5)P_2$:TF-$PI(4,5)P_2$ at a 97.4:2.5:0.1 molar ratio.

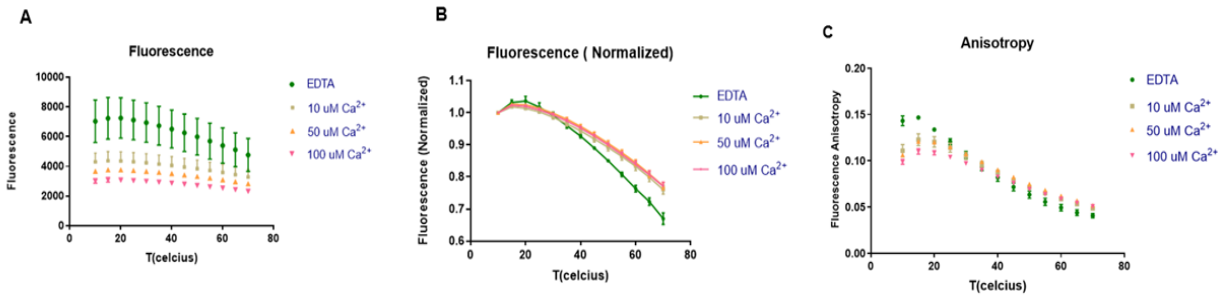

Figure 2 A,B- Impact of temperature on TF-PI(4,5)P_2 self-quenching; C- Impact of temperature on fluorescence anisotropy of TF-PI(4,5)P_2 fluorescence intensity**.** Excitation wavelength was 460 nm and the emission wavelength was set to 510 nm. All measurements were taken at range temperatures of 10 - 70 ºC.

Different calcium concentrations were also tested, namely 10, 50 and 100 µM Ca^{2+}.

At a given temperature, fluorescence self-quenching within the calcium-induced PI(4,5)P_2 and TF-PI(4,5)P_2 aggregates leads to further decreases in fluorescence intensity of TF-PI(4,5)P_2. This decrease is progressive as calcium concentration increases (Figure 2.B) and reflects the increase of the fraction of PI(4,5)P_2 fluorescent analogue within aggregates, as more calcium binds the membrane. In this way, at a given temperature, the fluorescence intensity is defined by the ratio of monomeric TF-PI(4,5)P_2/clustered TF-PI(4,5)P_2. Most of the fluorescence self-quenching is observed already at 10 µM Ca^{2+}, and more moderate changes are observed as calcium levels increase above this value, suggesting that PI(4,5)P_2 is already close to full incorporation in clusters at these calcium levels.

Recent results demonstrated that the clustered PI(4,5)P_2 exhibits significantly increased molecular order than the monomer[13]. This is also evident from the normalized fluorescence intensity (Figure 2.B), which shows that the monomeric TF-PI(4,5)P_2 is more sensitive to an increase in thermal-associated dynamics than the clustered molecules.

In order to confirm this observation, the temperature dependence of the fluorescence anisotropy (<*r*>) of TF-PI(4,5)P_2 was also evaluated.TF-PI(4,5)P_2 <*r*> values reflect fluorescence depolarization and in the absence of homoFRET would depend mostly on the dynamics of the system, which is expected to increase with temperature as a result of greater lipid mobility in the membrane. In this case, temperature increases are expected to induce a considerable decrease in fluorescence anisotropy of TF-PI(4,5)P_2. On the other hand, an additional source of fluorescence depolarization for this molecule is the presence of homo-FRET as its fluorescence emission show great overlap with its fluorescence excitation spectra, a pre-requisite for FRET to occur.

When calcium is added to the samples, a dramatic decrease in fluorescence anisotropy is observed, associated with increased FRET within calcium-dependent clusters [4,5].

At lower temperatures, the fluorescence anisotropy of PI(4,5)P_2 with EDTA is higher compared to the anisotropy values in the presence of calcium (Figure 2.C). This is due to the presence of homoFRET within Ca^{2+}/PI(4,5)P_2 clusters, which are absent when EDTA is present[4]. The increase in dynamics observed for monomeric PIP_2 at high temperatures, compensates for the absence of FRET, and at higher temperatures (above 45 ºC), the fluorescence anisotropy of the monomeric TF-PI(4,5)P_2 is actually lower than that of clustered TF-PI(4,5)P_2

These results confirm the recent observation that the order of lipids within the clusters is significantly higher than the order of monomers[13] and is less susceptible to temperature changes.

Considering the results observed for self-quenching, suggesting that temperature does not significantly affect the extent of PIP_2 aggregation between 20-70 °C, it is expected that FRET should not vary significantly with temperature as well. The observation that the variation of anisotropy with temperature is greater for monomeric PIP_2 than for aggregated PIP_2, suggests that the aggregated PIP_2 is less susceptible to the dynamic variations promoted by the increase in temperature. This result

confirms that the PIP_2 aggregates are more ordered than the "bulk" membrane as recently observed[13]

3.3. Effect of cholesterol in the formation of gel phase

3.3.1t-pna life-time

In order to clarify if cholesterol is able to inhibit the formation of gel phase by saturated $PI(4,5)P_2$, we performed experiments with the membrane probe trans-parinaric acid (tpnA) and with $(16:0)_2$ $PI(4,5)P_2$. The relative molar fraction of PIP_2 was kept constant (5% of total lipid), while the fraction of cholesterol was varied between 0% and 20%.

The fluorescence lifetime of tpnA is extremely sensitive to the presence of a lipid gel phase, as the membrane probe exhibits an unusual strong preference for incorporation in these solid phases. When incorporated in the gel phase, tpnA fluorescence lifetime increases dramatically, and this has been extensively employed as a marker for the formation of lipid gel phases[13–15].

In the absence of calcium, a short (< 4 ns) average fluorescence lifetime is observed for the different percentages of cholesterol (Figure 3), while in the presence of calcium, a marked increase in average fluorescence lifetime takes place, with recovered values above 25 ns.

From figure 3, it is clear that cholesterol, in the range analysed here, has no impact on the extent of lipid gel phase formed. This is considerably different from the impact of cholesterol on conventional lipid gel phases, which are triggered solely by acyl-chain packing. For $PI(4,5)P_2$, this means that if a sufficient concentration of saturated molecules are present at the plasma membrane, the formation of lipid gel nanodomains are likely to be inevitable, as intracellular divalent cation concentration is expected to be sufficient to drive clustering of all free $PI(4,5)P_2$.

3.4. Impact of PI(4,5)P2 gel phase formation on membrane permeabilization

As seen in previous results, cholesterol does not appear to influence $PI(4,5)P_2$ gel phase formation.

One possible outcome resulting from the presence of these nanodomains would be an

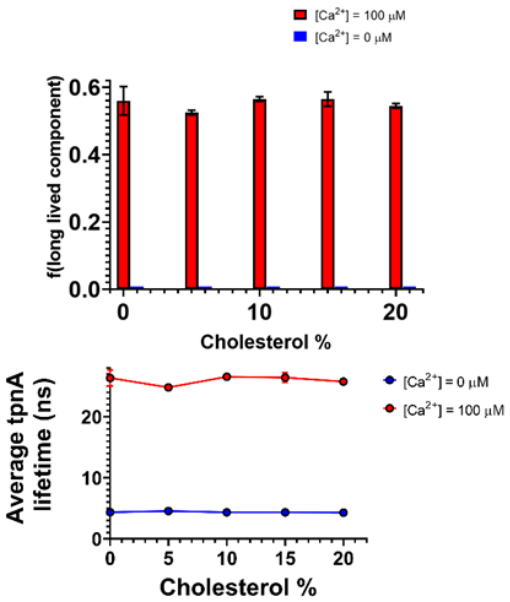

Figure 3 Fluorescence intensity weighed lifetime and fraction of total tpna fluorescence.$PI(4,5)P_2$ concentration was kept constant at 5%, while the composition of the other two components was varied.

increase in membrane permeabilization, with negative results for cellular integrity.

We investigated three different $PI(4,5)P_2$ acyl-chain configurations (Figure.4), so that the impact of gel-like nanodomains could be compared with the impact of unsaturated, fluid nanodomains.

Permeabilization levels obtained with different $PI(4,5)P_2$ species are very similar, and vesicles exhibited almost no permeabilization during the course of the experiment. Surprisingly, in the presence of EDTA, extensive permeabilization took place, also independently of lipid composition (Figure.4).

These results seem to suggest that EDTA interacts with lipid membranes increasing permeability, which was not expected. In any case, the results are clear in indicating that the $PI(4,5)P_2$ nanodomains do not promote significant permeabilization of the lipid membrane. This is also true for the gel domain-inducer 16:0 $PI(4,5)P_2$.

3.5. Membrane Tension

3.5.1 Manipulation of membrane tension

In order to induce changes in membrane tension, osmotic shocks were applied to GUVs. GUVs were prepared with a composition of 100% of POPC and 0.5 µM Flipper-TR probe.

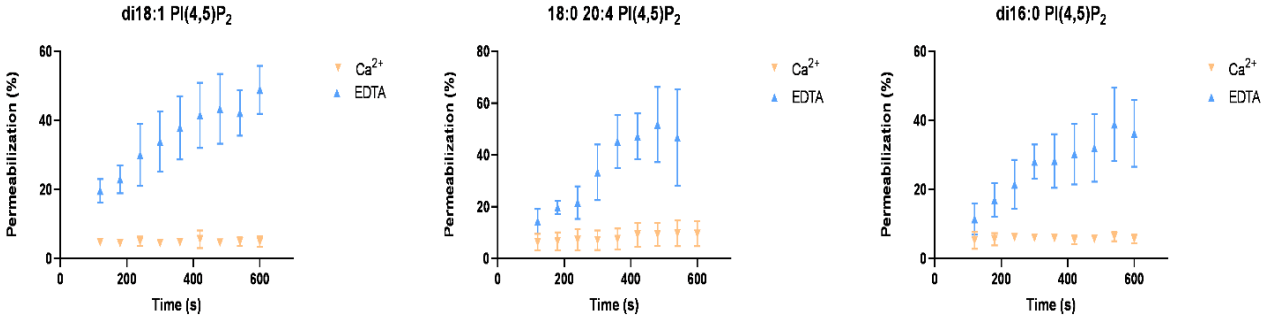

Figure 4 Permeabilization time traces for POPC:PI(4,5)P_2 95:5 (mol:mol) GUVs. The experiments were done for the three PI(4,5)P_2 acyl-chain compositions in study. The percentage of permeabilization values was measured in the presence (100 µM Ca2+, orange) and absence (5 mM EDTA, blue) of calcium. Results are the average of individual GUV permeabilization (N=6) and error bars correspond to standard deviations.

Sucrose concentration inside vesicles was always kept at 200 mM. Different concentrations of glucose in the outer vesicle environment were used to achieve different osmolarity differences.

An hyper-osmotic shock (Δosmolarity = 50 mOsm/L) was obtained using $[Glucose]_{outside}$ = 250 mM and hypo-osmotic shocks (Δosmolarity = - 100 mOsm/L) were obtained using $[Glucose]_{outside}$ = 100 mM. Iso-osmotic conditions (Δosmolarity = 0 mOsm/L) were obtained when $[Glucose]_{outside}$ = 200 mM. Osmolarity of each solution was always confirmed in an osmometer before the experiment.

Since Flipper-TR excited state lifetime is a good sensor for membrane tension, fluorescence lifetime imaging microscopy (FLIM) was employed to obtain individual measurements of Flipper-TR lifetime for each GUV.

As expected, upon a hyper-osmotic shock (ΔOsmolarity > 0), an increase in Flipper-TR fluorescence lifetime takes place (Figure 5). This is due to the decreased area per lipid produced by moderate contraction of the membrane, which increases packing pressure and favours alignment of the two dithienothiophene flippers of Flipper-TR. On the other hand, upon a hypo-osmotic shock (ΔOsmolarity < 0), a decrease in Flipper-TR fluorescence lifetime takes place, as the increase in membrane surface area leads to increased membrane tension with concomitant decreased lipid packing and lower alignment of Flipper-TR.

We can them be confident that the osmotic shock conditions chosen for generation of different membrane tensions are effective, and experiments on the behaviour of PI(4,5)P_2 in each scenario can be carried out with confidence in the future.

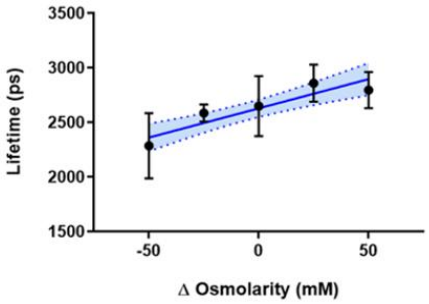

Figure 5 Flipper-TR lifetime vs ΔOsmolarity. ΔOsmolarity = $Osmolarity_{out}$ - $Osmolarity_{in}$. Results are the average of individual GUV permeabilization (N=7) and error bars correspond to standard deviations.

3.6. PI(4,5)P_2 incorporation and clustering in GUVs prepared from gel-assisted formation and from electroformation in Pt

GUVs can be obtained by gel-assisted formation or by electroformation in Pt. In order to ascertain if the method chosen had any impact on PI(4,5)P_2 clustering, both methods were studied. GUVs were composed of 95%POPC:0.5%PI(4,5)P_2:0.5%TF-PI(4,5)P_2.

There is a clear difference in TF-PI(4,5)P_2 intensity on the membrane of the GUVs prepared from electro- and gel-assisted formation. The gel-assisted method is the one that presents a greater intensity in the membrane (Figure 6.A). A likely justification for

the observation is the higher efficiency of incorporation of $PI(4,5)P_2$ when gel-assisted formation is employed.

The fluorescence lifetime of TF-$PI(4,5)P_2$ measured by FLIM is also moderately longer for the gel-assisted method of preparation for the GUVs (Figure 6.B), but the reasons in this case are less clear.

Since gel-assisted formation allow for more efficient incorporation of $PI(4,5)P_2$ into GUVs, all further experiments were carried out on GUVs prepared through this method.

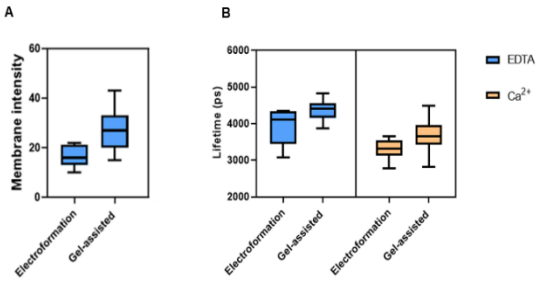

Figure 6 TF-$PI(4,5)P_2$ fluorescence intensity (A) and average lifetimes (B) on GUVs composed of POPC:$PI(4,5)P_2$:TF-$PI(4,5)P_2$ (99:0.5:0.5 molar ratio). Measurements were carried out through confocal fluorescence microscopy and FLIM, in the presence (orange)

3.7. Impact of membrane tension on $PI(4,5)P_2$ clustering

In order to evaluate $PI(4,5)P_2$ clustering, TF-$PI(4,5)P_2$ was employed, FLIM measurement were carried in POPC GUVs loaded with 0.1% or 0.5% of TF-$PI(4,5)P_2$, in the presence and absence of calcium.

Membrane tension changes were induced by adding solutions of different osmolarity to the GUVs prepared with 200mM sucrose. Surprisingly, TF-$PI(4,5)P_2$ fluorescence lifetime increases with osmolarity of the added medium. This is evident in the presence and absence of calcium, suggesting that the changes in fluorescence lifetime are not the result of clustering, as they are also observed for monomeric TF-PI(4,5)P2. (Figure 9).

When the difference in fluorescence lifetime in the presence and absence of calcium is calculated, results suggest that membrane tension plays no role in regulating $PI(4,5)P_2$ clustering, as this difference quantified in Figure 8, is somewhat constant, independently of the outer osmolarity, and hence independently of the membrane tension (Figure 7).

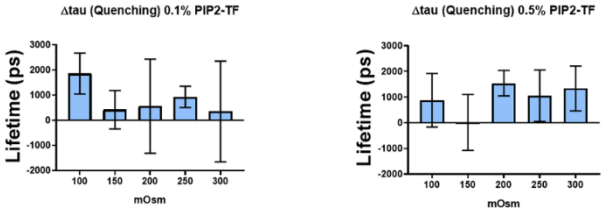

Figure 7 Difference in TF-$PI(4,5)P_2$ fluorescence lifetime in the presence and absence of calcium, for different osmolarity of the outer medium, reflecting different levels of membrane tension.

The exception is the sample measured with 100 mOsm in the external medium. However, the large difference in TF-$PI(4,5)P_2$ lifetime is more associated with the surprisingly large value of fluorescence lifetime recovered for monomeric TF-$PI(4,5)P_2$, and thus possibly is not reflective of a modified pattern for $PI(4,5)P_2$ clustering.

To test if increased permeabilization was responsible for this outlier, the same permeabilization measurements carried out before were tested for this osmotic shock conditions and compared with the results obtained for osmotic equilibrium (200 mOsm in the outer medium) (Figure 8).

Results clearly demonstrate that the excessive permeabilization observed in the presence of EDTA for both conditions are comparable. In this way, the TF-$PI(4,5)P_2$ outlier value obtained for 100 mOsm outer osmolarity is not the result of more efficient membrane permeabilization

4. Discussion

$PI(4,5)P_2$ exhibits a complex lateral organization at the plasma membrane, with considerable variability between cells types[16]. The presence of nanodomains enriched in the lipid will have considerable consequences for plasma membrane organization, as the protein profile and activity within these domains will be radically different from the bulk plasma membrane.

A strong tendency of $PI(4,5)P_2$ to stablish nanoclusters in the presence of divalent cation (Ca^{2+},Mg^{2+}) concentrations within physiological levels has been recently confirmed[4,9,17,18]. In this way, it seems that $PI(4,5)P_2$ is not entirely free for interaction when unbound from protein partners, but exists in a monomer-divalentcation induced cluster equilibria.

.

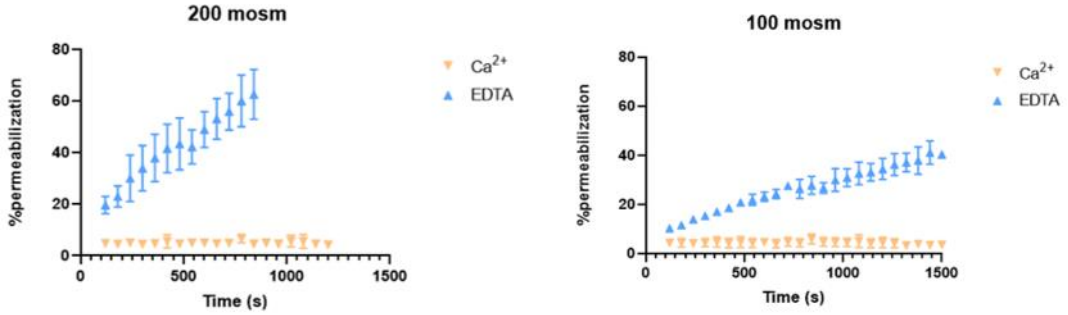

Figure 8 The carboxyfluorescein (CF) permeabilization study was carried out in GUVs composed of POPC:PI(4,5)P_2 95:5 mol:mol. The percentage of permeabilization values were measured in the presence (100 µM Ca^{2+}, orange) and absence (5 mM EDTA, blue) of calcium.

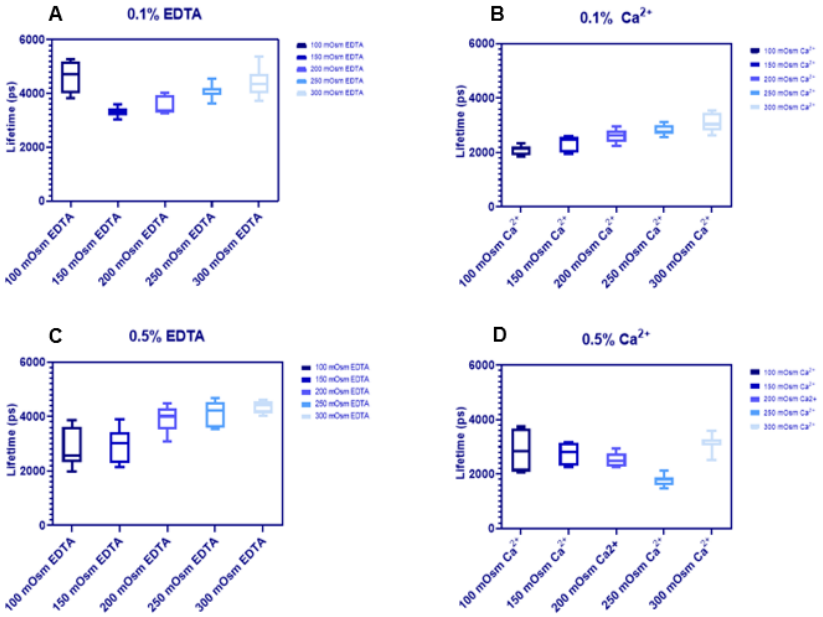

Figure 9 TF-PI(4,5)P_2 average fluorescence lifetimes in POPC GUVs**.** TF-PI(4,5)P_2 is present at 0.1 %(A and B) or 0.5 (C and D) % molar ratio, and FLIM measurements were carried out in the absence (A and C) and presence (B and D) of calcium. GUVs were prepared at 200 mOsm and the external solution osmolarity was changed from 100 - 300 mOsm.

Regarding the impact of temperature, both PI(4,5)P_2-divalent cation and multivalent PI(4,5)P_2-Ca^{2+}-PI(4,5)P_2 interactions were expected to be hampered by an increase in thermal-associated dynamics. Additionally, PI(4,5)P_2 membrane surface area was shown to be much more impacted by temperature than other lipid classes.

The result shown here indicate that in the range of 20-70 °C, temperature has almost no impact on the stability of calcium-induced PI(4,5)P_2 clusters. This is surprising, since other types of lipid phase separation observed in bio membranes are typically temperature dependent.

Significant changes in behaviour of the fluorescent analogue of PI(4,5)P_2 were evident when samples were cooled to 10 °C. Fluorescence intensity and anisotropy values decreased moderately at this temperature suggesting more efficient clustering and FRET within these clusters.

The impact of membrane tension on PI(4,5)P_2 clustering is more unpredictable. A recent study has identified PI(4,5)P_2 as the sensor for membrane tension changes in the plasma membrane[7]. Changes in plasma membrane tension lead to an enrichment of PI(4,5)P_2 in to specific domains, which then triggered a signalling response. However, the mechanism through which this occurred is still

obscure. Since changes in phospholipid surface area are observed when PI(4,5)P_2 interacts with either calcium or magnesium[19,20], it is conceivable that clustering of PI(4,5)P_2 could be impacted upon changes in lateral membrane pression. The results shown here seem to negate such an idea. In fact, the fluorescence lifetime of the PI(4,5)P_2 analogue remained roughly insensitive to different osmotic shocks which are expected to give rise to different degrees of membrane tension.

Clustering of 16:0 PI(4,5)P_2 has been recently show to induce the formation of a solid gel-like phase, even at extremely low concentrations of PI(4,5)P_2 (1%)[9]

Our results shown here also ruled out a role of cholesterol in mitigating the formation of these solid gel-like membrane domains. Since cholesterol was show not be ineffective in disrupting the formation of these phases, the presence of saturated PI(4,5)P_2 would invariably lead to the formation of undesirable gel phases at the plasma membrane. It is interesting then that this lipid is relatively rare. In fact, the dominant polyunsaturated PI(4,5)P_2 specie in animal cells, with 18:0,20:4 acyl-chains, might have been evolutionary selected to reduce ordering of PI(4,5)P_2 clusters, and in liposomes, the polyunsaturated PI(4,5)P_2 was shown to abrogate the formation of the 16:0 PI(4,5)P_2 gel phase[9], seemingly confirming this hypothesis.

Overall, the formation of PI(4,5)P_2 nanoclusters was shown to be largely insensitive to both physical and chemical factors tested. These results suggest that PI(4,5)P_2 clustering is not prone to regulation.

5. Ackowledgement

This document was written and made publically available as an institutional academic requirement and as a part of the evaluation of the MSc thesis in Biotechnology of the author at Instituto Superior Técnico. The work described here was performed at the Institute for Bioengineering and Biosciences (iBB)of Instituto superior Técnico (Lisbon, Portugal), during the period September-October 2020/2021, under the supervision of Doctor. Fábio Fernandes and co-supervised by Doctor. Sandra Pinto.

6. References

1. Borges-Araujo L; Fernandes F. Structure and Lateral Organization of Phosphatidylinositol 4,5-bisphosphate. *Molecules*. 2020;25(17):1-17.
2. Di Paolo G, De Camilli P. Phosphoinositides in cell regulation and membrane dynamics. *Nature*. 2006;443(7112):651-657. doi:10.1038/nature05185
3. Martin TFJ. PI (4 , 5) P 2 regulation of surface membrane traffic. *Curr Opin Cell Biol*. 2001;13(4):493-499.
4. Sarmento MJ, Coutinho A, Fedorov A, Prieto M, Fernandes F. Ca2+ induces PI(4,5)P2 clusters on lipid bilayers at physiological PI(4,5)P2 and Ca2+ concentrations. *Biochim Biophys Acta - Biomembr*. 2014;1838(3):822-830. doi:10.1016/j.bbamem.2013.11.020
5. Sarmento MJ, Coutinho A, Fedorov A, Prieto M, Fernandes F. Membrane order is a key regulator of divalent cation-induced clustering of PI(3,5)P2 and PI(4,5)P2. *Langmuir*. 2017;33(43):12463-12477. doi:10.1021/acs.langmuir.7b00666
6. Loh J, Chuang M, Lin S, Joseph J, Su Y, Hsieh T. An acute decrease in plasma membrane tension induces macropinocytosis via PLD2 activation. *J Cell Sci*. 2019;132:1-14. doi:10.1242/jcs.232579
7. Riggi M, Niewola-Staszkowska K, Chiaruttini N, et al. Decrease in plasma membrane tension triggers PtdIns(4,5)P 2 phase separation to inactivate TORC2. *Nat Cell Biol*. 2018;20(9):1043-1051. doi:10.1038/s41556-018-0150-z
8. Prieto JA, Estruch F, Córcoles-sáez I, et al. Pho85 and PI(4,5)P2 regulate different lipid metabolic pathways in response to cold. *BBA - Mol Cell Biol Lipids*. 2019. doi:10.1016/j.bbalip.2019.158557
9. Borges-Araújo L, Domingues MM, Fedorov A, Santos NC, Fernandes F. Acyl-chain saturation regulates the order of Phosphatidylinositol 4,5-bisphosphate nanodomains. *(submitted for publiciation)*. 2021.
10. Weinberger A. Gel-Assisted Formation of Giant Unilamellar Vesicles. *Biophysical*. 2013;105(July):154-164. doi:10.1016/j.bpj.2013.05.024
11. Angelova MI, Dimitrov DS. Liposome Electro formation. *Faraday Discuss Chem SOC*. 1986;81:303-311.
12. Loura LMS, Fedorov A, Prieto M. Partition of membrane probes in a gel/fluid two-component lipid system: a fluorescence resonance energy transfer study. *Biochim Biophys Acta*. 2000;1467(1):101-112. doi:10.1016/S0005-2736(00)00211-X
13. Borges-Araújo L, Domingues MM, Fedorov A, Santos NC, Fernandes F. Acyl-chain saturation regulates the order of Phosphatidylinositol 4,5-bisphosphate nanodomains. *(submitted for publciation)*.
14. Nyholm TKMM, Lindroos D, Westerlund B, Slotte JP. Construction of a DOPC/PSM/cholesterol phase diagram based on the fluorescence properties of trans -parinaric acid. *Langmuir*. 2011;27(13):8339-8350. doi:10.1021/la201427w
15. Silva L, De Almeida RFM, Fedorov A, Matos APA, Prieto M. Ceramide-platform formation and -induced biophysical changes in a fluid phospholipid membrane. *Mol Membr Biol*. 2006;23(2):137-148. doi:10.1080/09687860500439474
16. Sarmento MJ, Borges-Araújo L, Pinto SN, et al. Quantitative FRET microscopy reveals a crucial role of cyto-skeleton in promoting PI(4,5)P2 confinement. *Int J Mol Sci*. 2021;(in press).
17. Sarmento MJ, Coutinho A, Fedorov A, Prieto M, Fernandes F. Membrane Order Is a Key Regulator of Divalent Cation-Induced Clustering of PI(3,5)P 2 and PI(4,5)P 2. *Langmuir*. 2017;33(43):12463-12477. doi:10.1021/acs.langmuir.7b00666
18. Wen Y, Vogt VM, Feigenson GW. Multivalent Cation-Bridged PI(4,5)P2 Clusters Form at Very Low Concentrations. *Biophys J*. 2018;114(11):2630-2639. doi:10.1016/j.bpj.2018.04.048
19. Levental I, Janmey PA, Cēbers a, Cebers A. Electrostatic Contribution to the Surface Pressure of Charged Monolayers Containing Polyphosphoinositides. *Biophys\ J*. 2008;95(3):1199-1205. doi:10.1529/biophysj.107.126615
20. Bilkova E, Pleskot R, Rissanen S, et al. Calcium Directly Regulates Phosphatidylinositol 4,5-Bisphosphate Headgroup Conformation and Recognition. *J Am Chem Soc*. 2017;139(11):4019-4024. doi:10.1021/jacs.6b11760